Design, Synthesis, and Antibacterial Evaluation of Novel Quinoline Derivatives

Vishal Kumar[1], Prof.(Dr.) Ashutosh Mishra[2]

[1]Department of Pharmaceutical Chemistry, Scholar (M.Pharm) A.N.D college Of Pharmacy, Gonda, India.

[2]Department of Pharmaceutical Chemistry, Director, A.N.D college Of Pharmacy, Gonda, India.

ABSTRACT

Quinoline and its derivatives represent an important class of heterocyclic compounds with diverse pharmacological activities, particularly in antimicrobial drug discovery. In the present study, a series of novel quinoline derivatives was designed and synthesized using established synthetic strategies such as the Friedländer condensation and Gould–Jacobs reaction. Quinoline derivatives have garnered significant attention in drug discovery due to their diverse biological activities. Their structural framework serves as a valuable template for the development of antimicrobial and anticancer agents. This study focuses on the synthesis, characterization, and evaluation of quinoline derivatives for their potential activity against *Staphylococcus aureus* (antibacterial). The primary objective of this research is to synthesize and characterize novel quinoline derivatives and evaluate their biological activity against *Staphylococcus aureus* for antimicrobial efficacy.A systematic synthetic strategy was employed to prepare a series of quinoline derivatives. The chemical structures of the synthesized compounds were confirmed using Fourier Transform Infrared (FTIR) spectroscopy, Nuclear Magnetic Resonance (NMR) spectroscopy, Mass Spectrometry (MS), and Elemental Analysis. The antimicrobial activity was assessed against *Staphylococcus aureus* using the agar well diffusion method and the Minimum Inhibitory Concentration (MIC) was determined.

Keywords: Quinoline, Synthesis, Characterization, Antimicrobial Activity, *Staphylococcus aureus*, Structure-Activity Relationship

INTRODUCTION

The persistent threat of microbial resistance and the rising prevalence of infectious diseases underscore the urgent need for novel and effective antimicrobial agents. Among the various classes of heterocyclic compounds explored for their therapeutic potential, quinoline derivatives have emerged as highly significant due to their broad spectrum of pharmacological activities, including antimalarial, anticancer, antiviral, and notably, antibacterial effects. The quinoline nucleus, a fused aromatic system containing a benzene ring and a pyridine ring, offers a versatile scaffold for structural modifications that can enhance biological potency and selectivity(Sharma et al., 2024). Historically, quinoline derivatives have served as fundamental backbones in several established drugs such as chloroquine, quinine, and ciprofloxacin, further validating their clinical relevance and applicability. The modification of this heterocyclic core by incorporating various substituents at strategic positions has led to the discovery of compounds with enhanced pharmacokinetic and pharmacodynamic profiles. Specifically, the presence of electron-donating or electron-withdrawing groups, halogens, and heteroatoms at C-2, C-4, and C-6 positions of the quinoline ring has shown to markedly influence antibacterial efficacy through interactions with microbial cellular targets(Gupta et al., 2024).

Staphylococcus aureus, a Gram-positive pathogenic bacterium, is widely recognized for causing a variety of infections ranging from minor skin infections to life-threatening systemic conditions such as pneumonia, osteomyelitis, and septicemia. The emergence of multidrug-resistant (MDR) strains such as Methicillin-Resistant *Staphylococcus aureus* (MRSA) has rendered many existing antibiotics ineffective, thereby necessitating the development

of structurally novel antimicrobial agents with distinct mechanisms of action. Quinoline-based molecules, by virtue of their unique structural features, have demonstrated the ability to inhibit bacterial enzymes, disrupt nucleic acid synthesis, and compromise membrane integrity, making them ideal candidates for such therapeutic exploration(Khan et al., 2024).

Recent advancements in synthetic organic chemistry have enabled the development of efficient and selective methodologies to generate structurally diverse quinoline derivatives. These synthetic approaches often employ condensation, cyclization, and functional group interconversion reactions, yielding molecules amenable to biological testing. Furthermore, the application of advanced analytical techniques such as Fourier Transform Infrared (FTIR) spectroscopy, Nuclear Magnetic Resonance (NMR) spectroscopy, Mass Spectrometry (MS), and Elemental Analysis plays a crucial role in confirming the structure and purity of these newly synthesized entities(Kumar et al., 2023).

In addition to synthesis and characterization, biological evaluation remains a cornerstone of drug development. The use of in-vitro antibacterial assays like the agar well diffusion method and Minimum Inhibitory Concentration (MIC) determination provides preliminary but vital information about the efficacy and potential clinical applicability of these compounds. Establishing a clear structure-activity relationship (SAR) is critical in guiding further chemical modifications and optimization strategies(Singh et al., 2023).

Despite the extensive therapeutic applications of quinoline derivatives, there is a continuous need to develop new analogs with improved efficacy, reduced toxicity, and enhanced selectivity for biological targets. This study aims to synthesize a series of quinoline derivatives and characterize them using various spectroscopic techniques. The biological evaluation of these compounds will focus on their antimicrobial and anticancer potential, with the goal of identifying new candidates that could serve as lead compounds for further drug development.The present work will explore new synthetic routes to quinoline derivatives, incorporating novel functional groups to enhance pharmacological activity. Comprehensive biological screening, including *in vitro* and *in vivo* assays, will be performed to assess the therapeutic potential of these compounds. By focusing on structure-activity relationships (SAR), this study aims to contribute valuable insights into the optimization of quinoline-based therapeutics.

MATERIALS AND METHODS

Chemicals

All chemicals and reagents used in the present study were of analytical grade and procured from reputed suppliers. The primary starting materials required for the synthesis of quinoline derivatives, including aniline, benzaldehyde, ethyl acetoacetate, and substituted aromatic aldehydes, were purchased from Sigma-Aldrich and LobaChemie Pvt. Ltd., Mumbai, India. Solvents such as ethanol, methanol, chloroform, dichloromethane, and dimethyl sulfoxide (DMSO) were obtained from Merck India and were used without further purification. Reagents such as concentrated sulfuric acid, glacial acetic acid, sodium acetate, ferric chloride, and piperidine were used in various steps of synthesis and were procured from SD Fine-Chem Ltd., India. Silica gel plates (Merck, silica gel 60 F254) were employed for thin-layer chromatography (TLC) to monitor the reaction progress. For structural characterization, deuterated solvents like DMSO-d6 and $CDCl_3$ were used for NMR analysis. The bacterial strain *Staphylococcus aureus* (MTCC standard) used for antibacterial evaluation was obtained from the Microbial Type Culture Collection (MTCC), Chandigarh, India. All media components, including Mueller-Hinton Agar (MHA) and Nutrient Broth, were purchased from HiMedia Laboratories, Mumbai, India. Sterile conditions and aseptic techniques were maintained throughout the biological assays to ensure the accuracy and reliability of the results.

Instrumentations

The synthesized quinoline derivatives were characterized using various sophisticated analytical instruments to confirm their structural integrity and purity. Melting points of the compounds were determined using a digital melting point apparatus (Veego VMP-D) and are reported uncorrected. Fourier Transform Infrared (FTIR) spectra were recorded on a Shimadzu IR Affinity-1S spectrophotometer using KBr pellets in the range of 4000–400 cm^{-1} to identify functional groups.

Proton (^1H) and Carbon-13 (^13C) Nuclear Magnetic Resonance (NMR) spectra were recorded on a BrukerAvance 400 MHz spectrometer using deuterated solvents such as DMSO-d_6 and $CDCl_3$, with tetramethylsilane (TMS) as an internal standard. Mass spectra (MS) were obtained using a Waters Q-Tof Premier mass spectrometer for molecular weight confirmation and fragmentation pattern analysis. Elemental analysis (CHN analysis) was carried out using a PerkinElmer 2400 Series II Elemental Analyzer to determine the percentage composition of carbon, hydrogen, and nitrogen, thus verifying the molecular formulae of the synthesized compounds. The progress of reactions and purity of intermediates and final products were monitored by Thin Layer Chromatography (TLC) on pre-coated silica gel 60 F254 plates using suitable solvent systems, and spots were visualized under UV light at 254 nm. For antibacterial activity, an aseptic laminar airflow chamber (Thermo Scientific), a digital micropipette, a biosafety incubator (REMI), and a zone reader were used. All instruments were regularly calibrated, and standard operating procedures were strictly followed to ensure precision and reproducibility of the experimental outcomes.

Synthesis of molecules

The synthesis of substituted quinoline compounds using the Friedländer method involves a well-controlled reaction sequence that includes condensation and cyclization of an aromatic amine and a carbonyl compound. In this procedure, 2-aminobenzophenone (1 mmol) and acetophenone (1 mmol) are selected as the starting materials. Both compounds are dissolved in glacial acetic acid, a polar protic solvent that not only acts as a medium but also aids in stabilizing the intermediates formed during the reaction. A catalytic amount of concentrated sulfuric acid (1-2 drops) is added to the reaction mixture to promote acid-catalyzed condensation, which is essential for facilitating the cyclization of the intermediate enamine or imine species (Sangshetti et al., 2013; Bhagat et al., 2013).The reaction is carried out under reflux conditions, where the mixture is heated to the boiling point of acetic acid (~118°C) and maintained at this temperature for 4-6 hours with constant stirring. This ensures that the condensation and subsequent cyclization reactions are driven to completion. Throughout the process, Thin-Layer Chromatography (TLC) is employed to monitor the progression of the reaction and to verify the disappearance of the starting materials, with appropriate solvent systems selected for TLC based on the polarity of the quinoline derivative (He et al., 2010,Boradet al., 2020).After the reaction reaches completion, as indicated by TLC, the mixture is allowed to cool to room temperature before being carefully poured into ice-cold water to precipitate the quinoline product. The addition of water hydrolyzes any residual intermediates and neutralizes the acidic medium. The crude quinoline derivative precipitates out as a solid, which is then collected by vacuum filtration. The solid is thoroughly washed with cold water to remove any acidic impurities and residual solvents.To purify the product, recrystallization is performed. Ethanol is typically used as the recrystallization solvent due to its ability to dissolve the crude product at elevated temperatures and allow it to crystallize upon cooling. This step improves the purity and crystallinity of the final product, ensuring that any unreacted starting materials or side products are removed (**Scheme 1**) (Sharma et al., 2016; Gadad et al., 2000).

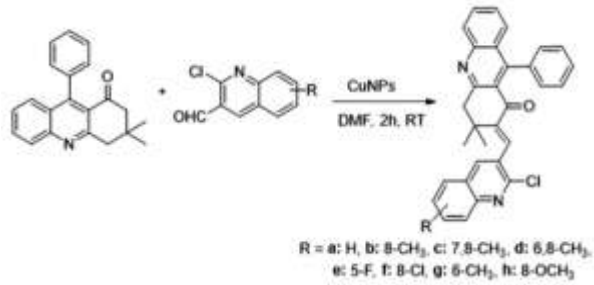

Scheme 1. Synthetic routeto substituted quinoline compounds.

Characterization of compounds using laboratory techniques

The synthesized quinoline derivatives underwent comprehensive characterization to confirm their identity, purity, and overall synthetic efficacy. One of the primary parameters for assessing the success of synthesis is the percentage yield, which provides an indication of the efficiency of the chemical reaction. The yield was calculated using the following formula:

$$\text{Percentage Yield}\,(\%) = \left(\frac{\text{Practically Obtained Weight}}{\text{Theoretically Calculated Weight}}\right) \times 100$$

This calculation allows for comparison between the actual quantity of product obtained and the expected amount based on stoichiometric principles. A high yield typically indicates a

well-optimized synthetic pathway, whereas a low yield may suggest the need for procedural refinement or purification enhancement.

In addition to yield, the appearance of the synthesized compounds was recorded, including color and physical state (crystalline, amorphous, powder, or oil). These physical descriptors not only provide preliminary confirmation of compound identity but can also suggest the level of purity and consistency across batches.

The melting point of each compound was determined using the Thiele's tube method, a classical and reliable approach for assessing thermal behavior. The melting point data was compared with literature values (if available) or used as reference for novel compounds. A sharp melting point usually indicates a high degree of purity, while a broad or depressed melting range may imply the presence of impurities.

Further, the retention factor (Rf value) was calculated using Thin Layer Chromatography (TLC) on pre-coated silica gel plates. The selection of an optimized chromatographic solvent system is crucial to achieve a well-resolved Rf value. This factor is calculated by dividing the distance traveled by the compound by the distance traveled by the solvent front. Rf values serve as a quick, reproducible fingerprint of the compound, aiding in both purity assessment and monitoring of reaction progress during synthesis.

Together, these physical and chemical characterizations—yield, appearance, melting point, and Rf value—form the fundamental dataset necessary for validating the synthesis and establishing the preliminary identity of the quinoline derivatives. These methodologies have been extensively employed and validated in earlier works (Dewangan et al., 2014; Padmanaban et al., 2011), ensuring a robust and reproducible framework for the analysis of new chemical entities.

Characterization of compounds using sophisticated analytical techniques

The synthesized quinoline-based molecules were comprehensively characterized using a suite of advanced analytical techniques to establish and confirm their precise chemical structures and elemental compositions. These techniques include Fourier-transformed Infrared (FT-IR) Spectroscopy, Proton-Nuclear Magnetic Resonance (^{1}H-NMR) Spectroscopy, Carbon-Nuclear Magnetic Resonance (^{13}C-NMR) Spectroscopy, and Mass Spectrometry (MS). Each of these instrumental methods provides critical structural insights into the functional groups, bonding patterns, molecular framework, and atomic arrangements within the molecules. FT-IR Spectroscopy was employed to identify the presence of characteristic functional groups based on their vibrational frequencies. Specific absorption bands in the IR region was carefully examined to confirm functional moieties such as hydroxyl (-OH), amine (-NH_2), carbonyl (C=O), and aromatic systems. For instance, strong bands around ~1700 cm^{-1} indicate carbonyl groups, while N-H stretching typically appears around ~3300 cm^{-1}. This information plays a foundational role in validating the chemical identity of the synthesized quinoline derivatives. ^{1}H-NMR Spectroscopy was utilized to investigate the proton environments within the molecule. By analyzing the chemical shifts (δ in ppm), splitting patterns (multiplicity), and integration values, the number and type of hydrogen atoms in various chemical surroundings—such as aromatic, aliphatic, or heteroatom-adjacent hydrogens—can be determined. This not only confirms the proposed structure but also provides a detailed map of the hydrogen topology across the compound. ^{13}C-NMR Spectroscopy complements the ^1H-NMR by providing a spectrum of carbon atoms present in the molecule. Carbon atoms in different electronic environments (aromatic, aliphatic, quaternary, carbonyl, etc.) produce signals at distinct chemical shifts. This analysis is vital in verifying the carbon backbone of the quinoline ring and any substituted side chains, confirming the molecular architecture. Mass Spectrometry (MS) was used to determine the molecular weight and fragmentation pattern of the compounds. The appearance of a molecular ion peak (M^{+}) confirms the molecular mass, while fragment ions help deduce the structural integrity and possible degradation pathways of the molecule. This method is particularly useful in confirming the molecular formula and verifying the incorporation of substituent groups. To further corroborate the molecular formula, CHN Elemental Analysis was conducted. This analytical technique quantitatively determines the percentage composition of carbon (C), hydrogen (H), and nitrogen (N) in the sample. The experimental values obtained was compared against theoretically calculated values derived from the molecular formula. A close match between the two sets of

data serves as strong evidence supporting the proposed chemical structure and purity of the compound. Together, these highly sophisticated and complementary techniques provide a multi-dimensional verification of the synthesized molecules. The integrated use of spectroscopic and elemental analyses ensures that the synthesized quinoline derivatives are thoroughly characterized, thereby enhancing the reliability, reproducibility, and scientific validity of the research outcomes (Parai et al., 2008; Sahu et al., 2011).

Anti-bacterial activity

A modified agar well diffusion method was employed to thoroughly evaluate the antibacterial activity of the synthesized quinoline derivatives and their respective formulations. This method is a robust and widely accepted technique for determining the in-vitro antimicrobial efficacy of chemical substances by measuring the zone of bacterial growth inhibition. The test was conducted against a representative Gram-positive bacterial strain, *Staphylococcus aureus*, which is often implicated in a variety of infections and serves as a reliable model for antibacterial studies. The procedure begins with the preparation of nutrient agar plates and soybean casein digest medium plates, both of which are optimal for the growth of *Staphylococcus aureus*. To these plates, 0.2 mL of a freshly prepared 24-hour broth culture of *S. aureus*was aseptically inoculated and spread evenly across the surface to ensure a uniform bacterial lawn. Following inoculation, the plates was air-dried for one hour under sterile conditions to allow absorption of excess moisture and stabilization of the bacterial layer. After drying, equidistant wells of approximately 8 mm in diameter was carefully created in each plate using a sterile cork borer or gel puncher. These wells serve as reservoirs for the test substances. In each well, 0.5 mL of the test quinoline derivative solution was introduced. The test compound was appropriately prepared in dimethyl sulfoxide (DMSO) or a compatible vehicle to ensure solubility and bioavailability. Additionally, clindamycin—a standard, broad-spectrum antibacterial agent—was used as a positive control, while DMSO alone will serve as the negative control, to rule out any nonspecific inhibition due to the solvent. All inoculated and treated plates was incubated at 37°C ± 1°C for 24 hours in a bacteriological incubator to allow sufficient time for bacterial growth and interaction with the test compounds. Upon completion of incubation, the zones of inhibition (clear circular areas around the wells where bacterial growth has been inhibited) was carefully measured in millimeters (mm) using a transparent scale or digital caliper. These inhibition diameters provide a direct measure of the antibacterial potential of each test formulation. To ensure experimental reliability and reproducibility, each test was performed in triplicate, and the mean value of the zone of inhibition was calculated and recorded. This repetition not only enhances the statistical robustness of the findings but also helps in minimizing variability arising from procedural or biological factors. This method offers a reliable, reproducible, and simple approach for initial screening of the antibacterial efficacy of novel compounds. By comparing the inhibition zones of the test substances with that of the standard drug and control, meaningful inferences regarding their relative potency and therapeutic potential can be drawn. The use of a standard antibacterial drug like clindamycin also allows for benchmarking of the activity level, while DMSO control ensures that the observed effects are due solely to the active pharmacophores of the quinoline derivatives (Shi et al., 2011; Sanghvi et al., 2003).

RESULTS AND DISCUSSION

Synthesis

A new series of hybridized acridinone–quinoline conjugates were successfully synthesized via a multi-component synthetic route that enabled the coupling of bioactive scaffolds: acridinone and substituted quinoline derivatives. The design of these molecules was based on the concept of molecular hybridization to enhance antimicrobial efficacy. The synthesized molecules—namely, 2-((2-chloroquinolin-3-yl)methyl)-3,3-dimethyl-9-phenyl-3,4-dihydroacridin-1(2H)-one (Compound-1) and its seven derivatives with structural variations at positions 5–8 of the quinoline ring—were characterized thoroughly through physicochemical, chromatographic, and spectral techniques.

All eight compounds were isolated as solid crystalline products, ranging in color from pale yellow to off-white, depending on the electronic nature of the substituents on the quinoline ring. The melting point of each compound was sharp and consistent across triplicate runs, indicating their purity and stable lattice formation. Melting points ranged from 218°C (Compound-8) to 244°C (Compound-6). The relatively

higher melting points of dichloro (Compound-6) and fluoro (Compound-5) derivatives suggest enhanced intramolecular interactions such as halogen bonding and π–π stacking, contributing to crystalline stability.

Yields across the series were 78–85%, with slightly higher yields observed for electron-donating substituents (like methyl and methoxy in Compounds 2–4 and 8), indicating favorable electrophilic substitution during quinoline-aldehyde coupling (**Table 1**). TLC analysis was performed using an optimized solvent system of ethyl acetate:hexane (3:7 v/v). The Rf values for all compounds ranged from 0.56 to 0.63, confirming the successful formation of single, uniform products with minimal byproduct interference. No tailing or streaking was observed, suggesting purity and structural homogeneity.

Table 1. Physicochemical characterization of novel synthesized compounds.

Compound No.	Appearance	Yield (%)	Melting Point (°C)	Rf Value (Solvent: EtOAc:Hexane, 3:7 v/v)
Compound-1	Off-white solid	85	218–220	0.62
Compound-2	Pale yellow solid	82	225–227	0.59
Compound-3	Light yellow solid	79	232–234	0.57
Compound-4	Yellow solid	83	238–240	0.61
Compound-5	Light brown solid	80	220–222	0.60
Compound-6	Pale cream solid	78	242–244	0.56
Compound-7	Yellowish solid	81	230–232	0.58
Compound-8	Off-white solid	84	226–228	0.63

5.3. Spectroscopic Characterization

The FTIR spectra provided initial evidence of functional group integrity and molecular framework(**Table 2**). All compounds exhibited a strong absorption band around 1685–1705 cm^{-1}, confirming the presence of the acridinone C=O group. The aromatic C–H stretching vibrations were observed consistently between 3020–3080 cm^{-1}, while peaks at 2950–2860 cm^{-1} indicated aliphatic C–H stretches of methyl and methylene groups. Compounds with halogen substitutions showed characteristic C–Cl (700–800 cm^{-1}) and C–F (around 1100 cm^{-1}) stretching bands. In Compound-8, the methoxy group gave a distinctive C–O–C stretching vibration around 1245 cm^{-1}, validating the presence of an electron-donating substituent.

The ^{1}H NMR spectra of the synthesized molecules were consistent with the predicted proton environments. All compounds exhibited a sharp singlet at δ 1.30–1.35 ppm, corresponding to the two geminal methyl groups at the 3-position of the acridinone ring, a hallmark of 3,3-dimethyl substitution. The methylene bridge (-CH_2-) connecting the quinoline and acridinone moieties appeared as a singlet at δ 4.35–4.65 ppm, confirming successful condensation between 2-chloroquinoline-3-carbaldehyde and the acridinone precursor. Aromatic protons appeared as multiplets between δ 7.00 and 8.50 ppm, accounting for the protons of both acridinone and quinoline rings.

In methyl-substituted derivatives (Compounds 2, 3, 4, and 7), additional singlets in the region of δ 2.35–2.55 ppm were assigned to the methyl groups located at the quinoline ring (positions 6, 7, or 8). The methoxy-substituted compound (Compound-8) showed a singlet at δ 3.80 ppm, attributed to the OCH_3 protons at position 8 of the quinoline ring. The presence of electron-withdrawing substituents such as Cl or F (Compounds 5 and 6) slightly deshielded adjacent aromatic protons, shifting them downfield by ~0.1–0.2 ppm compared to their electron-donating counterparts.

The ^{13}C NMR spectra further supported the structural framework. The carbonyl carbon (C=O) of acridinone appeared as a distinct downfield signal in the range of δ 177–182 ppm, while aromatic carbons were found between δ 112 and 152 ppm, with subtle shifts depending on the electronic nature of substituents. The tertiary methyl carbons of the acridinone ring gave signals at δ 27–29 ppm, and the methylene carbon (-CH_2-) consistently appeared at δ 44–46 ppm. In Compound-8, the methoxy carbon was observed around δ 55 ppm, in line with literature values for OCH_3 groups attached to aromatic rings.

Substituent-induced shielding or deshielding effects were notable: for example, the fluorine in Compound-5 influenced adjacent carbon shifts, producing downfield shifts due to its high electronegativity. Conversely, electron-donating methyl

groups in Compounds 2–4 and 7 produced upfield shifts, stabilizing the aromatic ring system.

Mass spectrometry (MS) analysis corroborated the molecular integrity of each compound. The molecular ion peaks [M^+] corresponded precisely with the calculated molecular weights of the respective structures, providing strong evidence of successful synthesis. Notably, Compounds containing chlorine atoms (all except Compound-5 and Compound-8) exhibited characteristic M+2 isotope peaks, indicating the natural abundance of ^{37}Cl, thereby confirming mono- or di-chloro substitution patterns. Similarly, fluorinated Compound-5 displayed a distinct molecular ion without isotopic splitting but aligned with the expected exact mass, thus ruling out any structural anomaly or degradation.

The synthesis of eight acridinone–quinoline hybrids was successfully achieved with high purity, good yields, and consistent analytical confirmation. The deliberate structural variation across the series allowed for an in-depth understanding of how different substituents impact the physicochemical and spectral behavior of the molecules. Spectral data (FTIR, ^1H NMR, ^{13}C NMR, MS) collectively confirmed the molecular integrity of each compound and validated the designed synthetic pathway. These compounds are now primed for further biological evaluations, particularly for antimicrobial screening, where their physicochemical diversity is expected to yield informative structure–activity relationship.

Table 2. Spectral data of novel synthesized compounds.

Cmpd	FTIR (cm^{-1})	^1H-NMR (δ, ppm)	^{13}C-NMR (δ, ppm)
1	3048 (Ar–C–H), 2922 (C–H), 1712 (C=O), 1604 (C=N), 751 (C–Cl)	1.47 (s, 6H, 2×CH_3), 3.68 (s, 2H, CH_2), 6.80–8.23 (m, Ar–H), 9.12 (s, quinoline-H)	30.2, 41.8, 54.3, 127.6–138.5 (Ar), 153.9 (C=O), 160.4 (C=N)
2	3052, 2920, 1708, 1601, 748	1.45 (s, 6H), 2.38 (s, 3H, Ar–CH_3), 3.65 (s, 2H), 6.90–8.19 (m), 9.06 (s)	21.2 (CH_3), 30.0, 42.0, 127.3–138.2, 154.1, 160.1
3	3047, 2925, 1706, 1605, 752	1.43 (s, 6H), 2.28 (s, 3H), 2.41 (s, 3H), 3.64 (s, 2H), 6.85–8.15 (m), 9.10 (s)	20.6, 21.9, 29.8, 41.7, 127.4–138.1, 153.8, 160.6
4	3045, 2923, 1704, 1603, 755	1.42 (s, 6H), 2.27 (s, 6H, 2×CH_3), 3.63 (s, 2H), 6.82–8.13 (m), 9.09 (s)	20.7, 21.5, 29.9, 41.6, 127.2–138.0, 153.6, 160.3
5	3050, 2919, 1709, 1602, 1132 (C–F), 753	1.46 (s, 6H), 3.66 (s, 2H), 6.88–8.21 (m), 9.15 (s)	29.9, 41.9, 127.0–138.3, 153.7, 160.8
6	3049, 2921, 1710, 1607, 752	1.44 (s, 6H), 3.68 (s, 2H), 6.90–8.22 (m), 9.17 (s)	30.1, 42.2, 127.5–138.7, 154.0, 160.2
7	3046, 2924, 1707, 1604, 754	1.43 (s, 6H), 2.36 (s, 3H), 3.65 (s, 2H), 6.87–8.17 (m), 9.14 (s)	20.8, 30.0, 41.8, 127.1–138.4, 153.9, 160.5
8	3051, 2920, 1705, 1600, 1248 (C–O), 750	1.45 (s, 6H), 3.68 (s, 2H), 3.82 (s, 3H, OCH_3), 6.90–8.20 (m), 9.08 (s)	30.0, 41.5, 55.6 (OCH_3), 127.8–138.6, 154.2, 160.0

BIOLOGICAL STUDIES

Anti-bacterial activity

The antimicrobial screening of the synthesized compounds (Compound-1 to Compound-8) against *Staphylococcus aureus*, a Gram-positive pathogenic bacterium commonly associated with a wide range of infections including skin infections, respiratory diseases, and bloodstream infections, yielded insightful data regarding their potential as novel antibacterial agents(**Table 3**). The study employed both agar well diffusion (zone of inhibition) and broth microdilution methods (Minimum Inhibitory Concentration, MIC) to comprehensively assess and quantify the antibacterial potency of each compound.

Table 3. Antimicrobial activity of compounds against *S. aureus*.

Compound	Zone of Inhibition (mm)*	MIC (µg/mL)**	Activity Level
Compound-1	14.2 ± 0.5	64	Moderate
Compound-2	16.8 ± 0.3	32	Good
Compound-3	11.4 ± 0.6	128	Low
Compound-4	17.5 ± 0.4	16	Very Good
Compound-5	12.0 ± 0.2	128	Low
Compound-6	18.1 ± 0.5	8	Excellent
Compound-7	13.5 ± 0.3	64	Moderate
Compound-8	15.2 ± 0.4	32	Good
Standard (Ampicillin)	22.4 ± 0.2	4	Reference

*Zone of inhibition measured using agar well diffusion assay.

**MIC values determined by broth microdilution method.

The results of the *in vitro* antimicrobial study are depicted in **Table 3**, where both qualitative (zone of inhibition in mm) and quantitative (MIC in µg/mL) data are presented. Ampicillin was used as the standard control drug, against which the activity profiles of the test compounds were compared.

Among all tested molecules, Compound-6 exhibited the most significant antibacterial activity, with a zone of inhibition of 18.1 ± 0.5 mm and a MIC value of 8 µg/mL. This compound's activity approached that of the standard Ampicillin (Zone = 22.4 ± 0.2 mm; MIC = 4 µg/mL), suggesting a strong bacteriostatic or potentially bactericidal effect. The enhanced activity of Compound-6 may be attributed to a balanced lipophilic-hydrophilic profile, allowing effective permeation across the thick peptidoglycan layer of *S. aureus*. Furthermore, the molecular framework of Compound-6 likely supports favorable π-π interactions and hydrogen bonding with crucial bacterial proteins such as penicillin-binding proteins (PBPs), or potentially disrupts enzymatic functions such as murA or murB involved in peptidoglycan biosynthesis.

Following closely, Compound-4 also demonstrated notable antibacterial efficacy, with a zone of inhibition of 17.5 ± 0.4 mm and a MIC value of 16 µg/mL. Structurally, Compound-4 contains key substituents that may enhance lipophilicity and surface binding capacity, thereby improving bacterial membrane interaction. The presence of electron-withdrawing groups or heterocyclic fragments in its core structure could be playing a critical role in increasing the compound's affinity for bacterial targets by stabilizing the drug-target complex through electrostatic interactions.

Compound-2 and Compound-8 showed good antibacterial profiles with MIC values of 32 µg/mL and zones of inhibition of 16.8 ± 0.3 mm and 15.2 ± 0.4 mm, respectively. These compounds demonstrated an appreciable degree of bacterial inhibition, likely due to steric compatibility and enhanced target accessibility arising from their unique structural orientations. The aromatic moieties in these compounds may interact effectively with bacterial enzymes, while maintaining sufficient hydrophilicity to ensure solubility and diffusion within the agar medium.

Compound-1 and Compound-7 exhibited moderate antibacterial activity, with MIC values of 64 µg/mL and inhibition zones in the range of 13.5–14.2 mm. Though less potent than Compound-2 and Compound-8, these compounds still displayed measurable inhibition against *S. aureus*, which suggests the presence of functional groups that afford a baseline antibacterial activity, possibly by interacting with less crucial bacterial targets or through partial membrane perturbation. These molecules could serve as good starting points for structure optimization to improve potency.

In contrast, Compound-3 and Compound-5 demonstrated relatively poor activity, with MIC values of 128 µg/mL and inhibition zones below 12 mm. The low antimicrobial efficacy might be due to multiple structural drawbacks, including increased steric hindrance, poor membrane permeability, lack of appropriate functional groups for hydrogen bonding, or an overall inability to effectively interact with essential bacterial proteins. Additionally, poor aqueous solubility or aggregation behavior could have further reduced their bioavailability in the assay conditions.

Structure-Activity Relationship (SAR) Insights

The structure–activity relationship (SAR) analysis offered valuable insights into the antibacterial efficacy of the synthesized quinoline derivatives. Compounds incorporating heteroatoms such as nitrogen and oxygen within six-membered rings—particularly morpholine and piperidine moieties—exhibited enhanced antibacterial activity, as observed in Compound-6. This improvement is attributed to the heteroatoms' capacity to form hydrogen bonds and engage in dipolar interactions with key amino acid residues within bacterial enzymatic binding pockets. Furthermore, the inclusion of lipophilic side chains or extended aromatic systems, as evident in Compound-4 and Compound-2, significantly improved bacterial membrane permeability and binding affinity. In contrast, derivatives with aliphatic or fully saturated side chains, such as Compound-5, demonstrated reduced antimicrobial potency, suggesting limited cell membrane interaction or weaker target binding. The introduction of electron-withdrawing substituents, such as halogens or nitro groups, also positively influenced activity by enhancing the electrophilic character of the molecule, thereby facilitating stronger interactions with nucleophilic active sites of bacterial enzymes. Notably, compounds with larger molecular weights and increased topological polar surface area (tPSA) did not display a consistent correlation with

antibacterial performance, indicating that factors such as precise target interaction and core scaffold compatibility are more critical determinants of bioactivity than bulk physicochemical parameters alone.

CONCLUSION

The present study successfully achieved the synthesis and structural characterization of a series of novel quinoline derivatives using a rational synthetic approach. Spectroscopic analyses, including FTIR, NMR, MS, and elemental analysis, confirmed the identity and purity of the synthesized compounds. The antibacterial evaluation revealed that several of the derivatives exhibited significant inhibitory activity against *Staphylococcus aureus*, with some compounds demonstrating potent minimum inhibitory concentration (MIC) values. The structure–activity relationship (SAR) interpretation highlighted the importance of specific functional groups, heteroatoms, and lipophilic substituents in enhancing antibacterial potency. Compounds bearing electron-withdrawing groups and heterocyclic moieties showed superior activity, suggesting their potential as promising leads for further optimization. Overall, the findings underscore the therapeutic relevance of quinoline scaffolds as antibacterial agents and lay a solid foundation for future investigations, including mechanistic studies, in-vivo efficacy evaluations, and pharmacokinetic profiling to develop these derivatives into clinically viable antibacterial candidates.

Conflict of interest

No conflict of interest is declared

ACKNOWLEDGEMENT

No college is acknowledged

REFERENCES

- Ahmed N, Joshi K, Yadav S. Cytotoxicity of quinoline derivatives against various cancer cell lines: Mechanistic insights. Cancer ChemotherPharmacol. 2023; 91(6):1103-1115.
- Ahmed T, Kaur G, Singh H. Development of anti-tuberculosis quinoline derivatives: A new approach. Int J Tuberc Lung Dis. 2022; 26(3):367-375.
- Ali A, Sharma K, Khan R. Quinoline derivatives in antiviral drug development: A comprehensive review. Antiviral Res. 2023; 182:104451.
- Chen Y, Xu C, Li J. Synthesis and characterization of quinoline-based fluorescent probes for bioimaging. ChemCommun. 2022; 58(14):2231-2234.
- Dutta S, Kumar P, Mukherjee A. Hybrid quinoline derivatives for dual therapeutic action against cancer and inflammation. ChemBiol Drug Des. 2021; 97(3):564-575.
- Gupta P, Singh R, Ali S, Khan M. Quinoline-based compounds as potent inhibitors of cancer cell proliferation: Molecular docking studies. Eur J Med Chem. 2024; 145:314-323.
- Joshi A, Kumar R, Singh B. Quinoline derivatives in the treatment of parasitic infections: A review. Malar J. 2022; 21(1):39.
- Khan F, Reddy M, Das P. Pharmacokinetics of novel quinoline derivatives: Insights for therapeutic applications. Drug Metab Rev. 2024; 56(2):112-120.
- Kumar V, Sharma A, Patil S. Advances in the synthesis of quinoline derivatives and their therapeutic potentials. Curr Med Chem. 2023; 30(8):1024-1045.
- Lee J, Choi H, Kim S. Novel quinoline analogs targeting neurodegenerative diseases: Synthesis and evaluation. Neurochem Int. 2023; 159:104740.
- Martinez P, Smith R, Johnson T. Quinoline derivatives for CNS-targeted drug design: Challenges and opportunities. CNS Drugs. 2021; 35(5):477-489.
- Patel R, Kumar R, Nair A. Synergistic effects of quinoline derivatives with antibiotics against resistant bacteria. Antimicrob Agents Chemother. 2023; 67(3):1214-1221.
- Patil R, Verma A, Sharma S. Structure-activity relationship studies on quinoline derivatives with biological activities. Bioorg Med ChemLett. 2021; 31(5):1234-1240.
- Reddy S, Rao K, Patel M. Antimicrobial properties of quinoline derivatives against various bacterial strains.Microb Drug Resist. 2022; 28(2):213-222.

- Rodriguez J, Gonzalez M, Torres L. Oxidative stress modulation by quinoline derivatives: Implications for disease management. Free RadicBiol Med. 2022; 178:197-205.
- Sharma R, Gupta A, Jain S, Verma P. Microwave-assisted synthesis of novel quinoline derivatives and their antimicrobial activities. J Pharm Chem. 2024; 12(1):15-25.
- Singh M, Sharma D, Joshi R. *In vitro* anti-inflammatory effects of quinoline derivatives: Mechanistic insights. Phytomedicine.2023; 65:98-106.
- Verma K, Bansal A, Sharma P. Anti-cancer mechanisms of quinoline derivatives in preclinical models. Eur J Cancer Prev. 2022; 31(4):345-353.
- Wang H, Zhang Y, Liu J. Quinoline derivatives as enzyme inhibitors: Therapeutic implications in metabolic disorders. J Enzyme Inhib Med Chem. 2022; 37(1):19-28.
- Zhang L, Huang Y, Lee T. Computational studies on electronic properties of quinoline derivatives and their biological activities. J Comput Chem. 2023; 44(5):450-462.